Structural and optical properties of ZnO nanoclusters supported on mesoporous silica

K. SOWRI BABU*, A. RAMA CHANDRA REDDY, CH. SUJATHA, K. VENUGOPAL REDDY, N. VENKATATHRI[a]
Department of Physics, Materials science laboratory, National Institute of Technology, Warangal-506 004, Andhra Pradesh, India
[a]*Department of Chemistry, National Institute of Technology, Warangal-506 004, A.P, India*

This paper reports on structural and optical properties of ZnO nanoclusters embedded in mesoporous silica (MPS) an inorganic host matrix. Small angle X-Ray Diffraction (SAXRD), Wide angle X-Ray Diffraction (XRD), N_2-Sorption (BET), Scanning Electron Microscopy/Energy Dispersive spectroscopy (SEM/EDS), Fourier Transform Infrared Spectroscopy (FT-IR), Ultraviolet – visible spectroscopy (UV–Vis.) and Photoluminescence (PL) spectroscopy were used to characterize the samples. The UV-Vis absorption and PL spectra show a strong blue shift due to the quantum confinement effect of ZnO semiconductor nanoparticles. On excitation with 318 nm light source, ZnO/MPS nanocomposite shows emission peaks at 344, 372, 455, 485 and 512 nm. The emission peaks at 372 and 485 nm are the contribution of mesoporous silica. The PL band at 344 nm is attributed to the band gap luminescence of ZnO which is smaller than the previous reports. We suppose that the emission at 455 nm is not the blue shifted green emission but it is due to the formation of Zn-O-Si bonds at the interface. Singly ionized oxygen vacancies in ZnO nanocrystals are responsible for the green emission at 512 nm.

(Received August 22, 2011; accepted September 15, 2011)

Keywords: Semiconductors, ZnO Nanocluster, Mesoporous silica, Optical properties

1. Introduction

The renewed interest in ZnO is due to its applications in fine photoelectronics, light emitting diodes, solar cell windows, acoustic wave devices, gas sensing and so on, owing to its direct wide band gap (Eg ~ 3.3 eV at 300 K), large exciton binding energy (60 m eV) and efficient radiative recombination [1,2]. The large exciton binding energy paves the way for an intense near-band edge excitonic emission at room temperature and even at higher temperatures. ZnO is one of the oxides that show quantum confinement effects in the usually accessible range of sizes, which results in the enlargement of the band gap with decreasing particle size [3]. Hence by preparing ZnO particles at nanometric scale, it would be possible to bring ZnO based electro-optic devices to very short wavelengths [3-5]. However, rather low chemical and temperature stability of nanoparticles usually results in distortion of originally adjusted parameters due to aggregation process or chemical reaction with their surroundings, thereby limiting practical applications of purely nanocrystalline systems. A well-known solution of the aggregation problem is encapsulation of nanoparticles in a chemically inert matrix [6]. Since its discovery in 1992 by Mobile research group, MCM-41 has become the most popular member of M41'S family of mesoporous silicates and aluminosilicate materials. Mesoporous silica seems to be the most challenging system for creation of nanocomposites owing to their possibility of preparing materials with different pore size (2-50 nm) and structure (hexagonal, cubic and lamellar phase) using different template molecules and concentrations [7-8].

Many strategies have been employed to incorporate ZnO in MPS host material including electrochemical deposition [9], static intercalation technique [6], and various impregnation methods [10, 11, 12, 13] but the UV emissions in PL spectra were not significantly blue-shifted relative to that of bulk ZnO. Furthermore, the visible luminescence of ZnO is still controversial because the synthesis procedure has great influence on photoluminescence properties [10, 14, 15, 16]. It is reported that the emission band at around 450nm is attributed to the blue shifted green emission which is due to the quantum confinement effects of smaller crystallite size of the ZnO nanoparticles inside the MPS host matrix [9, 12]. B. Yao et al. proved the existence of interactions between ZnO and Silica and these interactions will be destroyed when calcined at 350 ^oC for three hours to give rise to emissions at 420 and 470 nm. The unfamiliar violet PL band at 420 nm is related to the oxygen vacancies on the ZnO–SiO_2 interface traps and blue –green emission band have been detected by H. G. Chen et al. [15]. Y. Xiong et al. also reported that the emission peak at 405 nm is the blue shifted green emission [17]. W Zeng et al. studies show a broad PL spectrum ranging from 370 nm to 550 nm positioned at 420 nm owing to the blue shifted green emission [18]. Vaishnavi et al. observed the quenching of green emission and evolution of strong peak at around 405 nm along with UV emission [16] and assigned it to the interface interactions between ZnO and meoporous silica. Recently Shabnam et al. have studied

large number of samples and confirmed that the 410, 470 nm peaks appear only if the background is a-Si [19]. In the view of the existing literature, there is no correlation between the results it may be due to the different synthesis procedures employed that in turn effect the formation of defect state in the material. However, the influence of host media and its nature is also considerable [20]. So there is a need to study the optical properties of the ZnO nanoparticles incorporated in mesoporous silica.

In this article the synthesis and characterization of the ZnO mesoporous silica nanocomposite is presented. The structural, compositional and optical properties of the samples were investigated. Quantum confinement effects of the ZnO nanoparticles have been observed from both absorption and emission spectra. The origin of 455 nm emission along with green emission of ZnO nanocrystals is discussed.

2. Experimental procedure

Materials

The following materials were used for the preparation of the mesoporous silica (MPS) and ZnO/MPS. Tetraethyl orthosilicate (TEOS 98% Sigma Aldrich), cetyltrimethylammonium bromide (CTMABr, 98%, High Media) as a surfactant, Ammonia solution (extra pure, Sdfine), ethanol and Zinc Nitrate $6H_2O$ (99% Sdfine) were used.

Synthesis

Mesoporous silica was prepared by the method reported in [25]. The molar ratio of contents was adjusted to 1TEOS:0.152CTAB:21.8 NH_3:141.2 H_2O. The precipitate was filtered out and washed by distilled water to PH=7 and dried at 80 ºC for 12 h. The mesoporous silica is labeled as S_1. The procedure of incorporating ZnO into the channels of mesoporous silica is as follows: a 0.1M Zn $(NO_3)_2.6H_2O$ ethanolic solution was stirred at 30 ºC. The calcined mesoporous support materials (0.5g) were impregnated with 20 ml of 0.1 Zn $(NO_3)_2.6H_2O$ ethanolic solutions under vigorous stirring. Subsequently the materials were filtered and washed with methanol for several times and then transferred in an oven for aging at 80 ºC. The sample was calcined at 550 ºC for 1h (2 ºC/min) in air at ambient temperature and is labeled as S_2. Another sample is prepared with high weight percent of ZnO to confirm the presence of ZnO by XRD and is indicated as S_3.

3. Characterization

Small Angle X-ray powder diffraction (SAXRD) data were recorded on a Rigaku Ultima IV diffractometer using Cu K_α (λ=1.5405 A°) radiation in angular range from 1 to 6 (2θ). Measurements were done in the 2θ mode with a scanning speed of 0.02°/s in continuous mode. Wide angle XRD measurements were taken on Inel XRG 3000 diffractometer equipped with Cobalt K_α (λ=1.78897 A°) radiation (15 mA, 30 kV). Nitrogen adsorption isotherms were measured at 77 K in a Quantachrome surface area and pore size analyzer model NOVA 1200e. Prior to measurement run, samples were outgassed under high vacuum at 200 °C for few hours. Infrared spectra on KBr pellets were measured on a Shimadzu IR-408 infrared Spectrophotometer. The morphology was studied by JEOL JSM-6390 scanning electron microscope (SEM). Diffuse Reflectance UV–Vis absorption spectra were recorded on a Cary 5000 equipped with an integrating sphere in diffusion reflection mode. The PL measurements were carried out on Jobin Yuon spectrofluorometer, Model: FLUOROLOG - FL3-11. The Xenon arc lamp (450W) is used as the excitation light source in performing excitation and emission spectra.

4. Results and discussion

Structural analysis

The powder small angle X-ray diffraction patterns of MPS (S_1) and ZnO/MPS (S_2) nanocomposite are shown in Fig. 1. The decrease in peak intensity of S2 is attributed to the pore filling effects that can reduce the scattering contrast between the pores and the framework of mesoporous silica [18]. The change in the relative peak intensity and the small shift to higher 2θ values suggests that ZnO is present on the internal pore walls of mesoporous silica [22]. These results also demonstrate that the structure of mesoporous silica is unaltered even after the ZnO incorporation into pores of MPS [23]. At high loading of ZnO the complete loss of mesoporous structure is evident from the SAXRD pattern of the sample S3. The uptake of an aqueous zinc precursor is the sum of the solution occluded in the pores, corresponding in quantity to the total pore volume of the host matrix or slightly less [24]. A certain amount of the precursor will be drawn into the pores by capillary forces and becomes saturated. The excess solution causes ZnO formation on the external surface of the MPS or in other words it is incorporated interstitially in the MPS matrix, which causes lattice distortion. These lattice distortions will increase with concentration of the precursor and temperature. As the temperature increases, the size of the ZnO particles on external surface grows rapidly than those inside the pores, leading to the collapse of pore structure. The repeating distance a_0 between two pore centers has been calculated from SAXRD data using the formula $a_0 = 2d_{100}/\sqrt{3}$ for both S1 and S2. According to Grun et al. the pore diameter can be calculated from this value by subtracting 1.0 nm which is an approximate value for the pore wall thickness [25]. The pore diameters for S1 and S2 are 2.87 nm and 2.74 nm respectively.

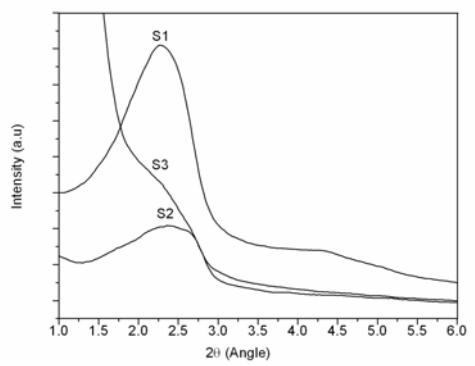

Fig. 1. Small angle X-ray diffraction patterns of MPS (S1), ZnO/MPS (S2) and ZnO/MPS with high content of ZnO (S3).

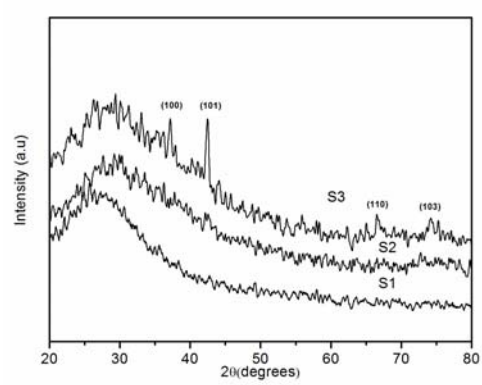

Fig. 2. Wide angle X-ray diffraction patterns of S1, S2 and S3.

Wide angle XRD results in Fig. 2 show no discernable changes in the diffraction patterns of S1 and S2. The ZnO nanoparticles will be too small or amorphous and could not be detected in S2 in this case. The XRD pattern of S3 unambiguously shows the prominent peaks such as (100), (101), (110), and (103) corresponds to ZnO wurtzite structure. It is reported that when the ZnO clusters formed are too fine i.e less than 3.5 nm, they may exist stably in the form of non-crystalline phase [26]. It shows that the ZnO clusters must reach critical size in order to have long range order. In the present experiment, the average size of the ZnO clusters formed may be greater than the critical size i.e 3.5 nm which is required to show crystalline nature.

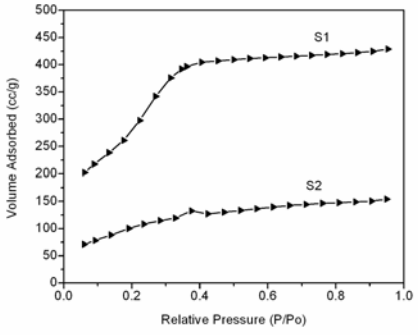

Fig. 3. N_2-adsorption isotherms of S1 and S2 measured at liquid nitrogen temperature (77K).

N_2 adsorption-desorption isotherms of S1 and S2 are indicated in Fig. 3. The specific surface area determined by the linear part of the BET equation (P/P_o=0.05-0.3) is 1185 m^2/g and 380 m^2/g for S1 and S2 respectively. This high surface area of MPS is due to the formation of smaller pores of diameter about 2 nm. The pore volume also drops from 0.66 to 0.24 cc/g. These results are in close agreement with the results reported previously [18]. The decrease in surface area and the pore volume confirms that ZnO was incorporated in the pores of MPS. The characteristic pore filling step of the isotherm nearly disappears after the formation of ZnO clusters, which indicates that most of the channels have been packed by ZnO clusters [18]. The pore diameters calculated for S1 and S2 using the formula $4V_p/a_s$ are 2.22 and 2.52 nm, where V_p is the specific pore volume and a_s is the specific surface area. A small increase in pore diameter 0.3 nm after impregnation of ZnO is due to the enhancement of the pore wall thickness. These results are consistent with the results obtained from SAXRD. The micrographs of MPS (S1) and ZnO/MPS (S2) taken by scanning electron microscope are shown in Fig 4. The inset is the SEM micrograph of S1 and it is evident from these micrographs that the MPS structure remains even after ZnO impregnation and ZnO is distributed uniformly inside the entire MPS. The amount of ZnO in S2 and S3 is about 11 and 19 % in weight, calculated according to the method reported by Bao et al. The SEM-Energy Dispersive Spectroscopy is used for further confirmation of ZnO presence in the composite. The amount of ZnO in S3 is estimated to be 16% in weight.

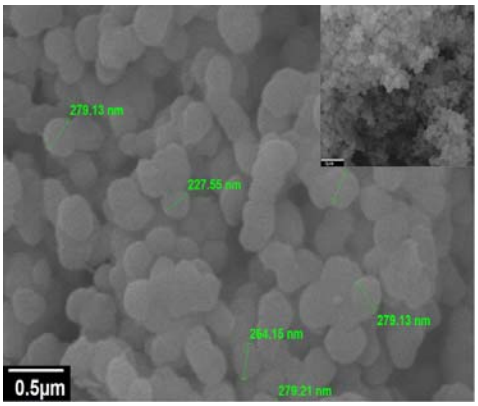

Fig. 4. Scanning electron micrographs of S1 (inset) and S2.

Optical characterization

The structure of S1 (bottom spectrum) and S2 (Top spectrum) are followed from FT-IR spectra, and the results are shown in Fig. 5. In MPS a broad peak centered at 3448 cm^{-1} corresponding to the stretching vibrations of –OH groups was observed, along with another distinct peak at 1635 cm^{-1} assigned to the bending modes of adsorbed water [27]. The absorption band at 1094 cm^{-1} is due to asymmetric stretching vibrations of Si–O–Si bridges. The

disappearance of the 964 cm^{-1} band and slight broadening of the 470 cm^{-1} band is observed in the S2. The latter should be attributed to the 447 cm^{-1} strong absorption band of ZnO. From the results of IR spectral measurement, it can be seen that the framework of MPS has been unaltered in the preparation process of ZnO nanoparticles, and the slight alternation of the spectrum is ascribed to the loading of trace amounts of ZnO [17]. The UV-vis diffusing reflectance spectra for S1 and S2 are shown in Fig 6. The MPS matrix shows no absorbance in this range and the optical absorption coefficient was obtained using the Kubelka–Munk function [6]. Sample S2 exhibits a strong absorption band at an absorption onset at about 285 nm and is shown in the inset of Fig. 6. This massive blue-shift to 285 nm in the absorption spectrum reflects an increasing band gap of the semiconductor which arises from the size quantization effect. The wavelength of absorption onset can be used to calculate the particle size of the ZnO clusters [15]. Haase et al. gave an empirical curve of absorption onset wavelength vs particle size, showing that the mean size of ZnO clusters at 10 Å corresponds to about 280 nm [4]. According to the Haase et al. the particle size of ZnO clusters corresponding to the optical absorption at 285 nm must be greater than 10 Å. The particle size of the ZnO crystallites in ZnO/MPS was estimated to be less than 1.8 nm and is in good agreement with previous reports [12, 15].

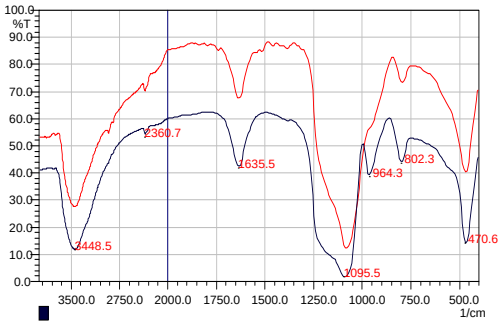

Fig. 5. FT-IR Spectra of S1 and S2 taken on KBr Pellets.

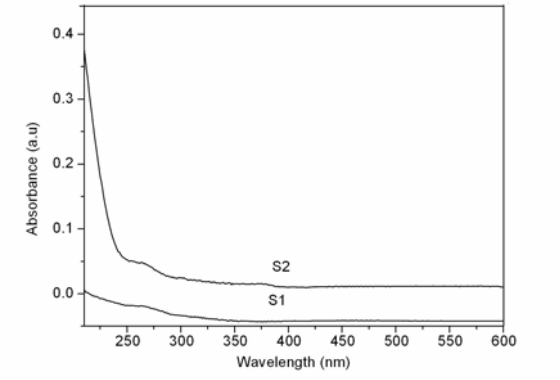

Fig. 6. Diffuse reflectance UV-Vis spectra of S1 and S2 taken by using $BaSO_4$ as the reference material.

The PL spectra were taken with an excitation wavelength of 318 nm for S1 and S2 and are shown in Fig. 7. In most cases the MCM-41emission is very weak, which may be obtained by continuous accumulation of the faint emission signal. Moreover, the intensity variation of the observed emission depends upon the preparation procedure and temperature [17]. In the case of our MPS, two strong and intense peaks at 375 and 477 nm were identified. The emission at 375 nm is due to the direct singlet-to-triplet excitation transition in the two-coordinated Si center and the later is due to the two folded coordinated silicon centers [28]. In general, ZnO will show much stronger and broader emission band which is situated in the green part of the visible spectrum, with a maximum between 500 and 530 nm (2.35-2.50 eV) [14] along with the UV emission. The emission band centered at 344 nm (3.60 eV) can obviously be assigned to band gap luminescence of ZnO nanoparticles grown inside the channels of the MPS matrix and is reported for the first time. Fig. 7 depicts that this peak has been strongly blue shifted when compared to the bulk ZnO band gap, attributed to the quantum confinement effect of ZnO nanoparticles in S2. This blue shift to short wavelength is much larger than that reported for ZnO nanoparticles incorporated into various mesoporous silica materials [16, 24, 26]. The emission peak at around 455 nm is rarely observed in ZnO/MPS composites. It is evident from the PL spectra that this emission is not the blue shifted green emission because green emission at 512 nm also exists in the same spectrum along with 455 nm emission peak is also detected. This result is contradictory to the earlier reports [9, 12, 17, 18]. The results of shabnam et al. have shown that the PL bands at 410, 470 nm are appearing only if the background is a-Si [19]. The green emission at 525 nm is also detected along with 410 and 470 nm peaks in the same spectrum almost in all the samples. From our PL results we suppose that the emission at 455 nm in this case is not due to singly ionized oxygen vacancies but due to the formation of O-Si-Zn bonds at the interface [19, 21]. The PL band at 512 nm is the green emission which is attributed to the singly ionized oxygen vacancies in the ZnO crystals [24].

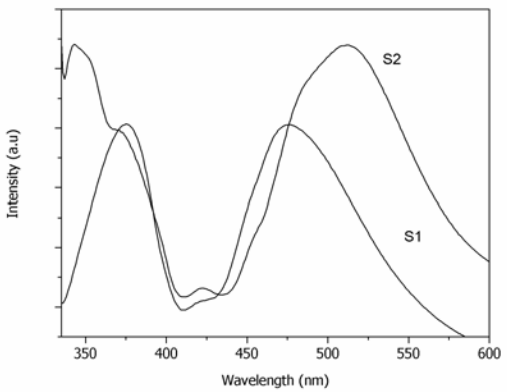

Fig. 7. Photoluminescence spectra of S1 and S2 taken at an excitation wavelength of 318 nm.

5. Conclusions

The structural and optical properties of ZnO/MPS nanocomposite are studied. The formation of nanoclusters of very small sizes less than 1.8 nm was observed. The preservation of the MPS structure even after impregnation is confirmed from SEM, SAXRD and FTIR. The absorption and emission spectra of ZnO/MPS show very strong blue shift. The emission peak at 344 nm is due to the band gap luminescence and is not reported so far. MPS shows two PL bands at 375 and 477 nm. ZnO nanoclusters in the composite show PL bands at 344,455 and 512 nm. The emission peak at 344 nm is attributed to the band gap luminescence. The 455 nm PL band is result of formation of Zn-O-Si bonds at the interface and another at 512 nm is due to singly ionized oxygen vacancies in ZnO.

Acknowledgements

The authors will be grateful to Dr. Venkatathri Narayanan, Department of Chemistry, NIT Warangal for his valuable suggestions. The authors thank Prof. Nalini, Head, Centre for research in nanotechnology, Karunya University, Coimbatore for providing PL measurements generously and Y. B. Ravi Shankar, University of Hyderabad for providing XRD facility.

References

[1] R. F. Service, Science **276**, 895 (1997).
[2] X. Y. Kong, Z. L. Wang, Nano. Lett. **3**,1625 (2003).
[3] U. Koch, A. Fotik, H. Weller, A. Henglein, Chem. Phys. Lett. **122**, 507 (1985).
[4] M. Haase, H. Weller, A. Henglein, J. Phys. Chem. **92**, 482 (1988).
[5] L. Fernandez, N. Garro, J. E. Haskouri, M. P. Cabero, J. A. Rodríguez et al, Nanotechnology **19**, 225603 doi: 10.1088/0957-4484/19/22/225603 (2008).
[6] L. I. Burova, D. I. Petukhov, A. A. Eliseev, A. V. Lukashin, Y. D. Tretyakov, Superlattices. Microst **39**, 257 (2006).
[7] N. K. Raman, M. T. Anderson, C. J. Brinker, J. Chem. Mater. **8**, 1682 (1996).
[8] J. Shi, Z. Hua, L. Zhang, J. Mater. Chem. **14**, 795 (2004).
[9] F. Gao, N. Chino, S. P. Naik, Y. Sasaki, T. Okubo, Thin solid films **495**, 68 (2006).
[10] B. Yao, H. Shi, H. Bi, L. Zhang, J. Phys. Condens. Mat. **12**, 6265 (2000).
[11] C. Cannas, M. Mainas, A. Musinu, G. Piccaluga Compos, Sci. Technol. **63**, 1187 (2003).
[12] W. H. Zhang, J. L. Shi, L. Z. Wang, D. S. Yan, Chem. Mater. **12**, 1408 (2000).
[13] F. Schro¨der, S. Hermes, H. Parala, T. Hikov, M. Muhler, R. A. Fischer, J. Mater. Chem, **16**, 3565 (2006).
[14] A. Van Dijken, E. A. Meulenkamp, D. Vanmaekelbergh, A. Meijerink, J. Phys. Chem B, **104**, 1715 (2000).
[15] H. G. Chen, J. L. Shi, H. R. Chen, J. N. Yan, Y. S. Li, Z. L. Hua et al. Opt. Mater **25**, 79 (2004).
[16] T. S. Vaishnavi, P. Haridoss, C. Vijayan, Mater. Lett, **62**, 1649 (2008).
[17] Y. Xiong, L. Z. Zhang, G. Q. Tang, G. L. Zhang, W. J. Chen, J. Lumin. **110**, 17 (2004).
[18] W. Zeng, Z. Wang, X. F. Qian, J. Yin, Z. K. Zhu, Mater. Res. Bull, **41**, 1155 (2006).
[19] Shabnam, C. R. Kant, P. Arun, Size and Defect related Broadening of Photoluminescence Spectra in ZnO:Si Nanocomposite Films. communicated available at arXiv:1007.2142.
[20] M. Bougerra, M. Samah, M. A. Belkhir, A. Chergui, L. Gerbous, G. Nouet, Chem. Phys. Lett, **425**, 77 (2006).
[21] Y. Y. Peng, T. E. Hsieh, C. H. Hsu, Appl. Phys. Lett. **89**, 211909 (2006).
[22] G. D. Mihai, V. Meynen, M. Mertens, N. Bilba, P. Cool, E. F. Vansant, J. Mater. Sci, **45**, 5786 (2010).
[23] F. Gao, N. Chino, S. P. Naik, Y. Sasaki, T. Okubo, Mater. Lett, **61**, 3179 (2007).
[24] N. Sathitsuksanoh, D. Wang, H. Y. Yang, Y. Lu, M. Park, Acta. Mater, **58**, 373 (2010).
[25] M. Grun, K. K. Unger, A. Matsumoto, K. Tsutsumi, Micropor. Mesopor. Mater **27**, 207 (1999).
[26] Q. Lu, Z. Wang, J. Li, P. Wang, X. Ye, Nanoscale. Res. Lett. **4**, 646 (2009).
[27] Q. Cheng, V. Pavlinek, Y. He, A. Lengalova, C. Li, P. Saha, Colloids and surfaces A:Physiochem Eng Aspects **318**, 169 (2008).
[28] J. L. Shen, C. F. Cheng, Curr. Opin. Solid St M, **7**, 427 (2003).

*Corresponding author: sowribabu@gmail.com